Pion femtoscopy measurements in small systems with ALICE at the LHC

Łukasz Graczykowski for the ALICE Collaboration
Faculty of Physics, Warsaw University of Technology

Physics motivation

Pion femtoscopy in p–Pb collisions

- Crucial test in the understading of physics of pA collisions - does collective expansion exist in pA collisions?
- Test of the validity of hydro [1, 2] and CGC scenarios [3].

Pion femtoscopy in Pb–Pb collisions

- Measure the size of the homogeneity region from which volume of the QGP can be inferred.
- Transverse momentum dependence of the radii a manifestation of strong collective motion of matter.
- Strong constraints on timescales and sensitivity to the EOS in dynamic models.

Pion femtoscopy in *pp* collisions

- Precise and differential data to address space-time characteristics of particle production in "elementary" collisions.
- Significant multiplicities, comparable to peripheral heavy-ions.

Analysis overview

Event selection

- ∼80 million minimum bias p–Pb collisions at $\sqrt{s_{\rm NN}}$ =5.02 TeV analyzed,
- Four multiplicity classes from V0A detector (0-20, 20-40, 40-60 and 60-90% defined as fractions of the analyzed event sample sorted by decreasing V0A signal). V0A acceptance: $2.8 < \eta < 5.1$.

Pion selection

- $0.12 < p_{\rm T} < 4.0$ GeV/c.
- $|\eta| < 0.8$.
- Track reconstruction by ITS & TPC.
- Particle identification by TPC & TOF.

Construction of correlation function

The correlation function C is defined experimentally as:

$$C(\mathbf{q}) = \frac{N_B^{pairs}}{N_S^{pairs}} \cdot \frac{S(\mathbf{q})}{B(\mathbf{q})}, \qquad (1)$$

where S (signal) is composed of pairs of particles from the same event and B (background) is composed of uncorrelated particles measured with the same single-particle acceptance (constructed using "mixing" method). Momentum difference $\mathbf{q}$ is evaluated in the Longitudinally Co-Moving System (LCMS) in which the total longitudinal pair momentum vanishes: $p_{1,\rm L} + p_{2,\rm L} = 0$. The three coordinates of $\mathbf{q}$ are then defined as follows: *long* - along the beam axis, *out* - along the pair transverse momentum, and *side* - perpendicular to the other two.

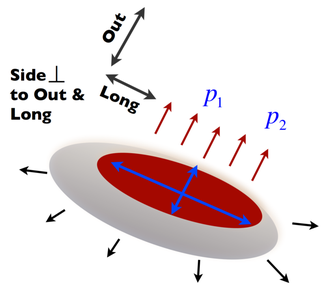

Non-femtoscopic correlations

Properties of non-femtoscopic structures

- Significant in small systems (ie. *pp*, p–Pb), practically negligible for central Pb–Pb collisions
- Wide structure in q (hundreds of MeV - much wider than femtoscopic signal)
- Different processes (eg. resonances, gamma conversion) contribute to the two-particle femtoscopic correlation function. Most significant include:
  - Jets represent most of the non-femtoscopic correlation for higher momenta
  - Minijets for lower momenta – Monte Carlo models should reproduce them and therefore the extraction of the pure femtoscopic correlation should be possible
- Jet/minijet hypothesis: growth of the non-femtoscopic correlations with increasing $k_{\rm T}$ and with decreasing multiplicity
- Observed in ALICE (*pp* [4]), STAR (*pp*, d–Au [5]) and other experiments

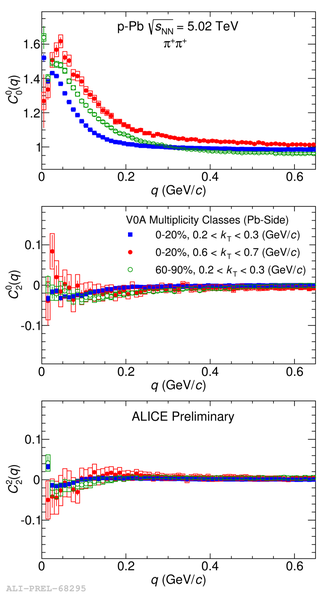

Figure 1: First three non-vanishing components of the SH representation of the $\pi^+\pi^+$ correlation functions for three multiplicity/$k_{\rm T}$ combinations, $l = 0$, $m = 0$ (top), $l = 2$, $m = 0$ (middle), and $l = 2$, $m = 2$ (bottom).

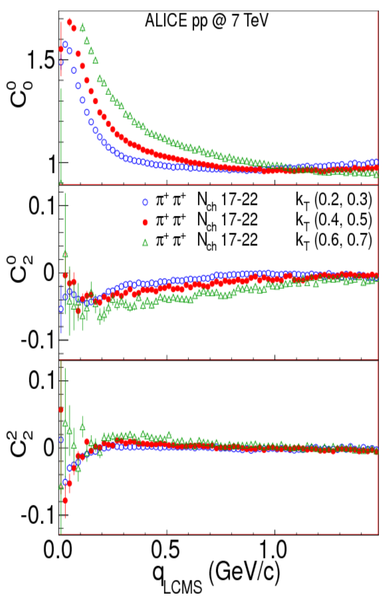

Figure 2: First three non-vanishing components of the SH representation of the $\pi^+\pi^+$ correlation functions from *pp* at $\sqrt{s} = 7$ TeV collisions for three $k_{\rm T}$ ranges and the same multiplicity range, $l = 0$, $m = 0$ (top), $l = 2$, $m = 0$ (middle), and $l = 2$, $m = 2$ (bottom). Figure from [4].

Fitting the correlation functions

Fitting procedure

- Non-flat baseline is clearly seen in the experimental data.
- Fitting procedure includes parameterization of non-femtoscopic correlations:

$$C(\mathbf{q}) = N C_{\rm f}(\mathbf{q}) C_{\rm B}(\mathbf{q}), \qquad (2)$$

where $C_{\rm f}(\mathbf{q})$ is the femtoscopic part and $C_{\rm B}(\mathbf{q})$, the non-femtoscopic part, is constrained from Monte Carlo models and N is overall normalization.

- Two Monte Carlo models used for parameterization of non-femtoscopic correlations:
  - EPOS 3.076 p–Pb at $\sqrt{s_{\rm NN}} = 5.02$ TeV (see Fig. 3),
  - PYTHIA Perugia-0 *pp* at $\sqrt{s} = 7$ TeV.

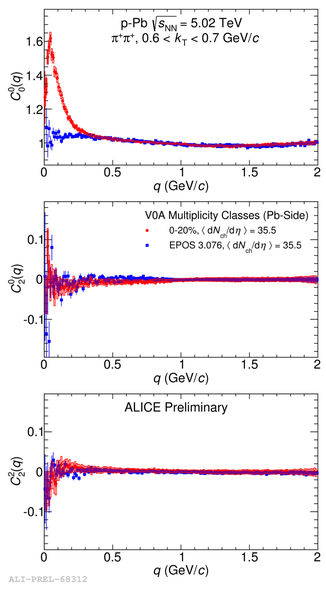

Figure 3: First three non-vanishing components of the SH representation of the $\pi^+\pi^+$ correlation functions for selected multiplicity and $k_{\rm T}$ range, compared to calculation from EPOS 3.076 model.

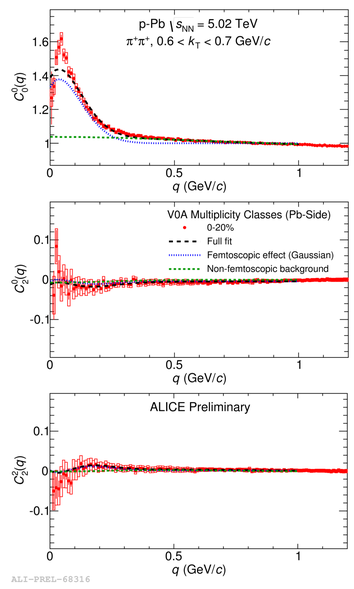

Figure 4: First three non-vanishing components of the SH representation of the $\pi^+\pi^+$ correlation functions for three multiplicity/$k_{\rm T}$ combinations, $l = 0$, $m = 0$ (top), $l = 2$, $m = 0$ (middle), and $l = 2$, $m = 2$ (bottom). The lines show the corresponding components of the fit (Gaussian fit).

Femtoscopic part

The space-time characteristics of the source are reflected in the correlation function via the integral equation:

$$C_{\rm f}(\mathbf{q}) = \int S(r, \mathbf{q}) |\Psi(\mathbf{q}, r)|^2 d^4 r, \qquad (3)$$

where r is the pair space-time separation four-vector. S is the source emission function (usually a 3D Gaussian). Ψ is the two-particle interaction kernel. For identical pions, in Bowler-Sinyukov approximation it gives:

$$C_{\rm f}(\mathbf{q}) = N\{(1-\lambda) + \lambda K_{\rm C}\left[1 + \exp(-R_{\rm out}^2 q_{\rm out}^2 - R_{\rm side}^2 q_{\rm side}^2 - R_{\rm long}^2 q_{\rm long}^2)\right]\}, \qquad (4)$$

where N is the overall normalization factor, λ is the fraction of correlated pairs, $K_{\rm C}$ is the Coulomb part of the two-pion wave-function (integrated over the spherical Gaussian source) and $R_{\rm out}$, $R_{\rm side}$ and $R_{\rm long}$ correspond the single-particle source size in LCMS in the *out*, *side*, and *long* directions, respectively.

Non-femtoscopic part

Fitting procedure includes the following parameterization of the non-femtoscopic correlations:

$$C_{\rm B}(\mathbf{q}) = C_{\rm f}\left[\left(1 + B_0^0(\mathbf{q})\right) Y_0^0 + \left(B_2^0(\mathbf{q}) + \gamma_2^0\right) Y_2^0 + \left(B_2^2(\mathbf{q}) + \gamma_2^2\right) Y_2^2\right] \qquad (5)$$

where Y are the shpherical harmonics, and B are the functions describing the non-femtoscopic correlation defined separately in each of the three non-vanishing SH components. B is: a Gaussian in B_0^0, a Gaussian in B_2^0 and a Gaussian plus additional linear function in B_2^2. Parameters of B were constrained from the analysis of Monte Carlo models.

Non-Gaussian fits

In the analysis of the *pp* system a study of the correlation function shape was performed and an alternative source shape that is a Lorentzian in *out* and *long* direction and a Gaussian in *side* was introduced [4]. The correlation function in that case has the following form:

$$C_{\rm f}(\mathbf{q}) = N\{(1-\lambda) + \lambda K_C\left[1 + \exp(-R_{\rm out}^{\rm E}|q_{\rm out}| - R_{\rm side}^2 q_{\rm side}^2 - R_{\rm long}^{\rm E}|q_{\rm long}|)\right]\}. \qquad (6)$$

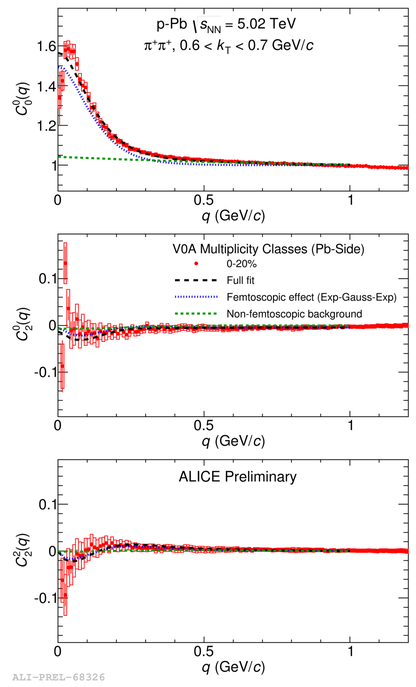

Figure 5: First three non-vanishing components of the SH representation of the $\pi^+\pi^+$ correlation functions for three multiplicity/$k_{\rm T}$ combinations, $l = 0$, $m = 0$ (top), $l = 2$, $m = 0$ (middle), and $l = 2$, $m = 2$ (bottom). The lines show the corresponding components of the fit (Exp-Gauss-Exp fit).

Source sizes

- Radii universally decrease with $k_{\rm T}$,
- Slope of this decrease is similar for all multiplicities in *out* and *long* directions, and is visibly increasing with multiplicity in the *side* direction,
- All radii grow with event multiplicity.
- Non-Gaussian shape better describes experimental correlations.

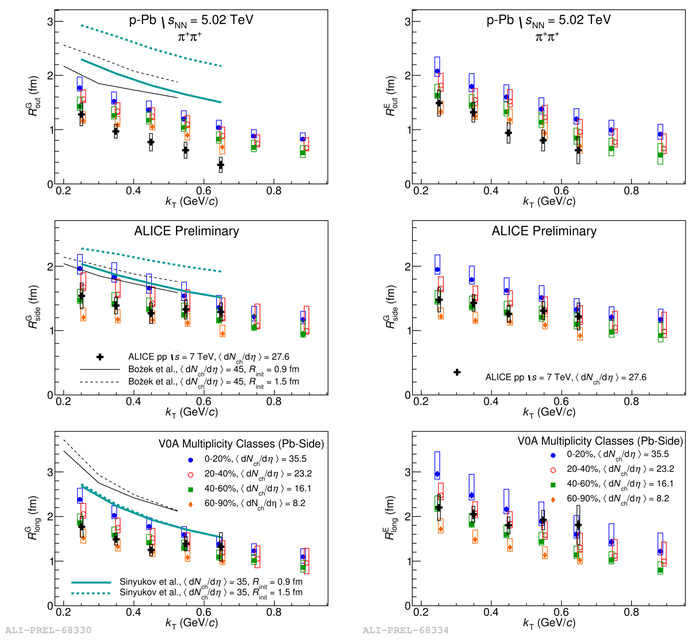

Figure 6: Femtoscopic radii (results of Gaussian fit) as a function of the pair transverse momentum $k_{\rm T}$ for four multiplicity classes. For comparison, radii from high-multiplicity *pp* collisions and four predictions for p–Pb are shown as crosses and lines, respectively. Top panel shows $R_{\rm out}$, middle panel shows $R_{\rm side}$, bottom panel shows $R_{\rm long}$. The points for multiplicity classes 20-40% and 40-60% have been slightly shifted in $k_{\rm T}$ for visibility.

Figure 7: Femtoscopic radii (results of Exp-Gauss-Exp fit) as a function of the pair transverse momentum $k_{\rm T}$ for four multiplicity classes. For comparison, radii from high-multiplicity *pp* collisions are shown as crosses. Top panel shows $R_{\rm out}$, middle panel shows $R_{\rm side}$, bottom panel shows $R_{\rm long}$. The points for multiplicity classes 20-40% and 40-60% have been slightly shifted in $k_{\rm T}$ for visibility.

Comparison with hydrodynamic calculations

- Two calculations assuming the existence of a collectively expanding system [1, 2].
- Both models employ two initial transverse size assumptions: $R_{\rm init} = 0.9$ fm and $R_{\rm init} = 1.5$ fm.
- Charge particle multiplicities are comparable to ALICE 0-20% multiplicity class.
- Scenarios with lower initial size are closer to the data, but still above.
- Slope of the $k_{\rm T}$ dependence is comparable between all versions of the calculation and the data
  - $R_{\rm out}$ predictions are universally higher than the measured radii.
  - For $R_{\rm side}$ the calculations are in good agreement, both in magnitude and in the slope of the dependence, with the data for highest multiplicity.
  - $R_{\rm long}$, calculations by Bożek are significantly higher (at least 30%) than most central data, while Sinyukov is only slightly higher.

Comparison of 2- and 3-pion radii in Pair Rest Frame

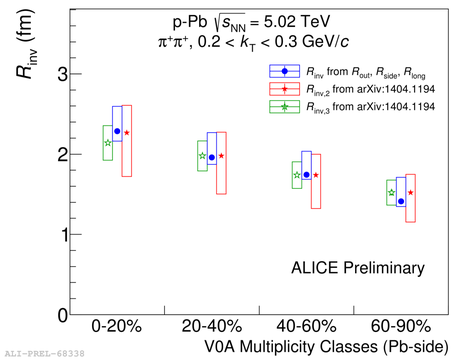

Figure 8: Comparison of 1D radii in Pair Rest Frame extracted from 3D radii in Longitudinal Co-Moving System (Gaussian fit) with 1-dimensional 2-pion and 3-pion correlation analysis from [6].

Summary

- Three-dimensional pion femtoscopic radii in LCMS have been measuerd in p–Pb collisions at $\sqrt{s_{\rm NN}}$=5.02 TeV.
- Radii were found to decrease with $k_{\rm T}$ in all cases, similar to measurements in AA and high multiplicity *pp* collisions.
- Data are compared at high multiplicity to predictions from two distinct models, each of them based on the mechanism of a fast hydrodynamic expansion of the created medium.
- Models predict too large values of the $R_{\rm out}$ and $R_{\rm long}$ parameters, however the introduction of smaller initial size brings calculations closer to data.
- $R_{\rm side}$ parameter and the slope of the dependence of all radii on $k_{\rm T}$ is described in a satisfactory way.
- Models based on the CGC formalism without a hydrodynamical stage predict similar sizes in p—Pb as compared to those in *pp* data. This is observed for low multiplicity collisions, where the differences between *pp* and p–Pb datasets are within 10% [3].

Bibliography

[1] P. Bożek and W. Broniowski.
Phys.Lett., B720:250–253, 2013.

[2] V.M. Shapoval, P. Braun-Munzinger, Iu. A. Karpenko, and Yu. M. Sinyukov.
Phys. Lett. B, 725:139–147, 2013.

[3] A. Bzdak, B. Schenke, P. Tribedy, and R. Venugopalan.
Phys.Rev., C87(6):064906, 2013.

[4] K. Aamodt et al. (ALICE Collaboration)
Phys.Rev., D84:112004, 2011.

[5] M.M. Aggarwal et al. (STAR Collaboration)
Phys.Rev., C83:064905, 2011.

[6] B. Abelev et al. (ALICE Collaboration)
arXiv: 1404.1194 [hep-ex], 2014.

HUMAN CAPITAL
NATIONAL COHESION STRATEGY

This work has been supported by the European Union in the framework of European Social Fund through the Warsaw University of Technology Development Programme, realized by Center for Advanced Studies as well as by the Polish National Science Centre under decisions no. DEC-2011/01/B/ST2/03483, DEC-2012/05/N/ST2/02757. The author is a scholar within Sub-measure 8.2.2 Regional Innovation Strategies, Measure 8.2 Transfer of knowledge, Priority VIII Regional human resources for the economy Human Capital Operational Programme co-financed by European Social Fund and state budget.

EUROPEAN UNION
EUROPEAN
SOCIAL FUND